Ukrainian Journal of Ecology

Ukrainian Journal of Ecology, 2018, 8(1), 194–210 doi: 10.15421/2018_204

ORIGINAL ARTICLE

Assessment of uncertainty associated with precipitation and temperature predictions: climate change impact assessment in Lenjanat Watershed, Central Iran

Afrooz Bagheri*[1], Bahram Malek Mohammadi[2], Banafsheh Zahraie[3], Amir Hessam Hasani[4], Farzam Babaie[5]

[1]Faculty of Environment and Energy, Islamic Azad University, Science and Research Branch, Tehran, Iran.
E-mail: afrooz_bagheri@yahoo.com
[2]Faculty of Environment, University of Tehran, Iran.
[3]School of Civil Engineering, College of Engineering, University of Tehran, Tehran, Iran.
[4]Department of Technical and Engineering, Science and Research Branch, Islamic Azad University, Tehran, Iran.
[5]Department of Technical and Engineering, Science and Research Branch, Islamic Azad University, Tehran, Iran.
Submitted: 12.12.2017. Accepted: 27.01.2018

The most popular method for predicting future behavior of global climate system under various greenhouse gas emission scenarios is using General Circulation Models (GCM). This study aims at predicting local climate change impacts on average rainfall and temperature in Lenjanat watershed in Iran in the period of 2006-2035. For this purpose, after performing trend analysis using Mann-Kendall test, the output data of general circulation models of atmosphere with two scenarios of climate change, i.e. 8.5 and 4.5, were down scaled with LARS-WG model at the Pol-Kalleh station. The results of that synoptic station were assessed for the fundamental period 1975-2005 and the future period of 2005-2035. To assess the model power, root mean square error and absolute error were calculated between monitored and modeled data. Models were appropriate for Lenjanat watershed station. And finally, data uncertainty was investigated. Results show that rainfall is decreasing and maximum and minimum temperature is increasing in both scenarios. Humid days are decreasing, but arid days are increasing. The maximum decrease in humid days was in November and increase in arid days was in May. More decrease in humid days and more increase in dry days happened in the pessimist scenario. There was a high correlation between rainfall, river flow rate, and underground water level.
Key words: climate change; Lenjanat watershed; Mann- Kendall; general circulation models of atmosphere; LARS-WG

Introduction

Climate change is among the biggest challenges human has ever faced. Climate change has extensive impacts on earth climate system. The most important impacts affect atmosphere, hydrosphere, hemisphere ice, and biosphere. Undoubtedly, human activity will increase in years and decades to come, hence, greenhouse gases in the atmosphere will increase, which in turn, changes the earth climate variables. Even if greenhouse gas emissions stop right now, climate variables continue to change. This will severely influence water, agriculture, and energy systems. (Hasheminasab et al., 2013).

Despite recent improvements in GCMs capabilities in modeling climate change, such models still suffer from serious difficulties in generating temperature and daily rainfall data (Trigo, Palutikof, 2001). In fact, when GCM models are used, outputs of numerical models of general circulation of atmosphere should be downscaled (Salon et al. 2008). LARS-WG, one of the most well-known models for generating accidental weather data, is used to generate rain fall values, radiation, maximum and minimum daily temperatures in a station under fundamental and future climate conditions (Semenov, 2002). This model can model past and future periods, but requires a special climate scenario for each period. This model can also be used for modeling lost data and statistical gaps. Also, estimating climate change at local or district level is associated with a large number of different uncertainty resources analyzed in this study. Najafi and Babaian (2008) in a recent study on climate change in Iran, have compared daily output of ECHO-G global model in the future and past. They have designed a climate scenario for the district based on the model spatial resolution power and ran Lars model based on ultimate micro scale scenario. Meshkatee et al. (2010) analyzed Lars power in simulating Golestan meteorology data from 1993 to 2007 and reached to the conclusion that

the most errors in simulated data by the proportion model was about real data related to sunny time variable and the rainfall, maximum and minimum temperature variables were simulated carefully. Abbasi et al. (2010), Bovani and Varid (2005), Khazanedari et al. (2009), Mehdizadeh et al. (2011) are among the other studies in this domain. Guo et al. (2012) predicted temperature change in Yangtze River Basin using ASD model for climate change conditions and found that rainfall will decrease in 2020s in all parts of district, while it will increase in Yangtze River Basin in 2050s and 2080s.

Methods

Lanjanat watershed with an area of 1100 km^2 is located 51°8 ′ to 51°45′E and 32°2′ to 32°24′N. It is a semi-arid area. It covers Lenjan and Mobarakeh, and some parts of city of Shahreza in Isfahan Province in central part of Iran. In this basin, Zayandehrood River and Shoor River, as well as several small rivers, lead surface runoffs into the exit point of the basin. Due to the average annual rainfall and temperature in Lenjanat (187.2 mm and 14.8℃), this area is placed in the arid group based on De Martonne's climate classification scheme. We presented the Lenjanat climate properties (Table 1) and geography of the area in Isfahan Province – see Fig. 1 (Afraz Cunsulting Engineers, 2015).

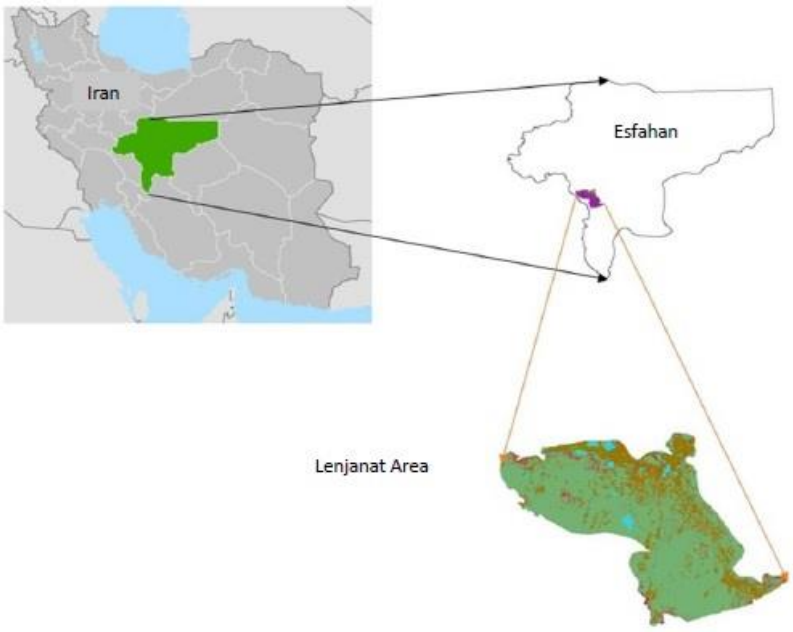

Fig. 1. Geography of Lenjanat Area

Table 1. Climate Properties of Lenjanat

Climate change	De Martonne's climate factor	Minimum Annual rainfall (mm)	Maximum Annual rainfall (mm)	Long-term average annual rainfall(mm)	Maximum of absolute Annual temperature(℃)	Minimum of absolute Annual temperature(℃)	Annual average temperature(℃)
arid	7.5	58.5	329	187.2	41.5	-15.5	14.8

Table 2. Monthly Temperature and Rainfall in Lenjanat Area, 1975-2005

	Sunny Hours	Temperature	Rainfall
January	6.81	3.3	11.07
February	7.59	4.6	11.30
March	7.74	8.8**5**	13.42
April	8.68	13.71	10.09
May	10.17	18.31	4.36
June	11.49	22.78	0.75
July	11.30	25.67	0.24
August	10.83	24.75	0.83
September	10.03	21.53	0.06
October	8.24	16.03	1.61
November	6.88	10.35	9.42
December	6.41	5.37	13.78

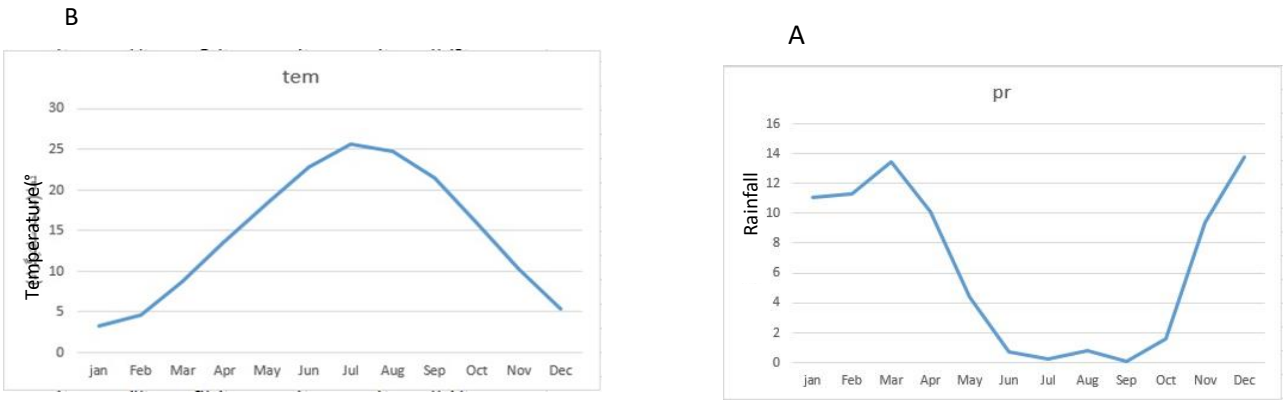

Fig. 2. Average Monthly Rainfall (A) and Average Monthly Temperature (B), in the Lenjanat Area (1975- 2005)

According to Table 2 and Figure 2 and 3, the maximum temperature, rainfall, and sunny hours in the Lenjanat Area were in June, December, and March and minimum temperature, rainfall, and sunny hours were in January, June, and December.

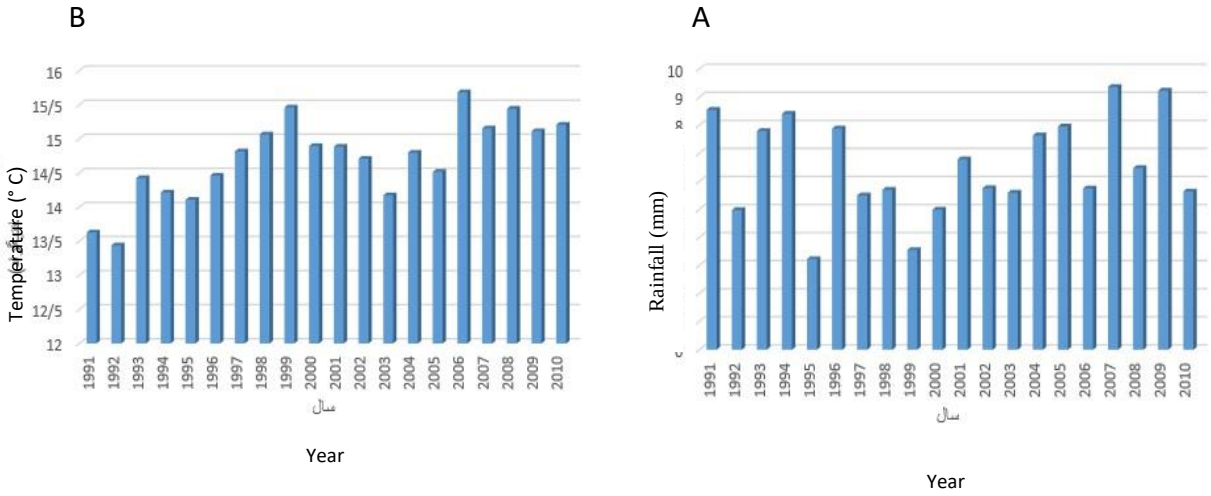

Fig. 3. Rainfall (A) and temperature (B) in in the Lenjanat Area (1991-2010).

Frequency of Humid and Arid Days

Daily rainfall data in the spring, the summer, the fall, and the winter are categorized into arid days and humid days. Determining humid and arid days are done based on humidity threshold (less than 0.1 mm is called arid days and more than that is called humid days)

General Circulation Models

Intergovernmental Panel on Climate Change has employed new "Representative Concentration Pathways" (RCPs) scenarios as representatives of key lines of greenhouse gases in its 5th report. The above scenarios are based on properties of different levels of technology and socio-economic conditions, and future policies that can emit different levels of greenhouse gases thus cause climate change. Different RCP scenarios are based on different radiative forcing levels, which in turn, are due to greenhouse gases. In this study we have utilized RCP 4.5 and 8.5. (Salon et al., 2008).
RCP8.5 scenario (pessimistic): in the case of not adopting policies of decreasing effects and coping with climate consequences, it is predicted that Earth climate will follow RCP8.5 emission scenario. In this scenario population will be 12 billion by 2100 when carbon dioxide density will be 1960 (per million).
This process will continue up to 8.5 w/m^2 radiative forcing in 2100. (Salon et al., 2008).
RCP4.5 scenario (optimistic): in this scenario, carbon dioxide density will be 750 (in million) by 2100 and radiative forcing of greenhouse gases before that time will be fixed to 4.5 w/m^2. In this scenario, population growth rate is low, but so is the rate using of new energy and technology (Salon et al., 2008). A new version of the LARS-WG incorporates predictions from 15 GCMs used in the IPCC AR4 (Salon et al. 2008). Table 2 summarises important features of these GCMs.

Table 3. Global climate models from IPCC AR4 incorporated into the LARS-WG stochastic weather generator

Oceanic resolution	Atmospheric resolution	Model Institute (Country)	MODEL
1.25 × 1.25° L20	2.5 × 3.75° L19	Handley Weather Forecast Center (UK)	HadCM3
1.5 × 1.5° L40	T63 L31	Max Planck Institute for Meteorology (Germany)	ECHAM5-OM
0.8 × 1.9° L31	T63 L18	CSIRO Seafarer Research (Australia)	CSIRO-MK3.0
0.3–1 × 1° L50	2 × 2.5° L24	Geophysical Fluid Dynamics Laboratory (USA)	GFDL-CM2.1
0.5–2 × 2.5° L23	T42 L30	Meteorological Research Institute (Japan)	MRI-CGCM2.3.2
0.3–1 × 1° L40	T85 L26	National Center for Atmospheric Research (USA)	CCSM3
0.5–2 × 2° L31	T63 L45	National Center for Meteorologiques Research (France)	CNRM-CM3
0.2 × 0.3° L47	T106 L56	Climate System Research Center (Japan)	MIROC3.2
2 × 2° L31	2.5 × 3.75° L19	Institut Pierre Simon Laplace (France)	IPSL-CM4
4 × 5° L13	4 × 5° L20	Goddard Institute for Space Studies (USA)	GISS-E-R
0.5–1.5 × 1.5° L35	T63 L31	Bjerknes Climate Research Center (Norway)	BCM 2.0
1.9 × 1.9° L29	T47 L31	Canadian Center for Climate Modelling and Analyzing (Canada)	CGCM3 T47
0.5–2.8 × 2.8° L20	T30 L19	Meteorological Institute of the University of Bonn (Germany)	ECHO-G
2 × 2.5° L33	4 × 5° L21	Institute of Mathemitics (Russia)	INMCM 3.0
0.5–0.7 × 1.1° L40	T42 L26	National Center for Atmospheric Research (USA)	NCARPCM

Investigating Trend

An increase in global temperature has changed climate parameters: rainfall, evaporation, and transpiration that in turn have affected river flow. Trend identification is an important issue in hydrological time series analysis, but it is also a difficult task due to the diverse performances of methods, in other words before analysis and modeling and the probable trend of data deletion and stationary. Trend identification is a required task in hydrological series analysis, because it is the basis not only for understanding the long-term variations of hydrological processes, but also for revealing periodicities and other characteristics of hydrological processes (Fang Sang et al. 2014).

A number of parametric and non-parametric tests have been applied for trend detection. Both parametric and non-parametric tests are commonly used. Parametric trend tests are more powerful than nonparametric ones, but they require data to be independent and normally distributed. On the other hand, non-parametric trend tests require only that the data be independent and can tolerate outliers in the data. One of the widely used non-parametric tests for detecting trends in the time series is the Mann -Kendall test. The Mann-Kendall trend test is derived from a rank correlation test for two groups of observations proposed by Kendall (Hamed and Rao 1998). Parametric and non-parametric tests share independent data. The Mann–Kendall test, which is widely used to detect trends in hydrologic data, is modified to account for the effect of scaling (Hamed 2007). That is more appropriate for the identification of trends in time series of hydrological variables. (Khaliq et al. 2009). Null hypothesis for the Mann-Kendall test is that the data are independent and randomly ordered, i.e. there is no trend or serial correlation structure among the observations. However, in many real situations the observed data are auto correlated. The autocorrelation in observed data will result in misinterpretation of trend tests results. Cox and Stuart (1955) state that: 'Positive serial correlation among the observations would increase the chance of significant answer, even in the absence of a trend.' A closely related problem that has been studied is the case where seasonality exists in the data (Hamed and Rao 1998). Von storch (1995) suggested pre-whitening method in which removing autocorrelation impact of Mann-Kendall can be done by removing data series correlation impact. They removed data autocorrelation impacts in trend analysis with Mann-Kendall method by correcting the amount of variance and presenting TFPW method.

Z statistics was done in one of the following ways:

$$Z = \begin{cases} \frac{S-1}{\sqrt{var(s)}} & if \quad s > 0 \\ 0 & if \quad s = 0 \\ \frac{S+1}{\sqrt{var(s)}} & if \quad s < 0 \end{cases} \qquad (1)$$

Where

$$Var(s) = n(n-1)(2n+5) - \sum_t t(t-1)(2t=5)/18 \quad (2)$$

$$S = \sum_{k=1}^{n-1} \sum_{j=k+1}^{n} sgn\binom{n}{k}(x_j - x_k) \quad (3)$$

$$sgn(\theta) = \begin{cases} 1 & if \quad \theta > 0 \\ 0 & if \quad \theta = 0 \\ -1 & if \quad \theta < 0 \end{cases} \quad (4)$$

$$|z| \leq Z\alpha/2 \quad (5)$$

Null hypothesis indicated that it's irregular and no trend. It means that Z isn't significant statistically. (For instance there isn't heat and coldness: Null hypothesis is accepted. −Zα/2 < Z < Zα/2 or dry and wet period) If $|z| \leq Z\alpha/2$ Amount of Zα/2 is standard deviation (Z of table). Rival hypothesis indicates that it Z < −Zα/2 or if Z > Zα/2 trended. It means that Z is significant statistically. If Rival hypothesis is accepted (Fu et al 2004). This trend is |Z | > 1.64, | Z | > 1.9, and |Z | > 2.58 at the confidence levels of .90, .95, and .99 respectively.

LARS-WG Exponential Micro-Scale Model

New interest in local stochastic weather simulation has arisen as a result of climate change studies. At present, output from global climate models (GCMs) is of insufficient spatial and temporal resolution and reliability to be used directly in impact models. A stochastic weather generator, however, can serve as a computationally inexpensive tool to produce multiple-year climate change scenarios at the daily time scale which incorporate changes in both mean climate and in climate variability (Semenov, Barrow, 2002).

For future modeling, model should know statistical behavior of monitoring period. Statistical behavior are real monitored data including minimum temperature, maximum temperature, rainfall and sunny hours. So, at first, in the observation period, properties of each station including name, location, altitude and daily meteorology data files were to be taken as inputs for the model. Then, LARS-WG model, was used for analyzing data which resulted in a summarized text file that includes statistical properties of observation data as monthly and seasonal averages for the whole period. Based on the trend of time series observation data, model regenerates station data in this period and then compares simulated monthly data averages and observation data are compared using statistical tests and charts to assess model capability in simulating meteorology data. After assessing model capability in generating data for future period in each station, climate change scenario file should be developed for the studied location based on the general circulation models of atmosphere and should be defined for the model (Semenov, Barrow, 2002).

Predicting future data will be done by this 4-stage model:

1. Analyzing fundamental data: analyzing statistical properties of observation data for determining data statistical features.
2. Initial data generation: generating artificial data for the model in the fundamental period and determining statistical properties of artificial data.
3. Statistical comparison: adapting and comparing statistical properties of observation data and artificial generated data.
4. Generating daily data in future: using statistical properties of fundamental data and greenhouse gas emission scenarios and outputs of general circulation models in generating daily time series transferred to future with the same statistical properties of fundamental data.

Model receives fundamental data of the monitored period and extract their statistical properties and runs the model for the fundamental statistical period to ensure its validity and capability and regenerate artificial data in the fundamental period. Finally, outputs are compared using Chi-square, t-test, and F-tests with the help of 30-year observational statistics to evaluate the model's performance in data reconstruction. (Semenov, Barrow, 2002).

It utilizes semi-empirical distributions for the lengths of wet and dry day series, daily precipitation and daily solar radiation. The semi-empirical distribution Emp= { a0, ai; hi, i=1,....,10} is a histogram with ten intervals, [ai-1, ai), where ai-1 < ai, and hi denotes the number of events from the observed data in the i-th interval. Random values from the semi-empirical distributions are chosen by first selecting one of the intervals (using the proportion of events in each interval as the selection probability), and then selecting a value within that interval from the uniform distribution. Such a distribution is flexible and can approximate a wide variety of shapes by adjusting the intervals [ai-1, ai). The cost of this flexibility, however, is that the distribution requires 21 parameters (11 values denoting the interval bounds and 10 values indicating the number of events within each interval) to be specified compared with, for example, 3 parameters for the mixed-exponential distribution used in an earlier version of the model to define the dry and wet day series.

The intervals [ai-1, ai) are chosen based on the expected properties of the weather variables. For solar radiation, the intervals [ai-1, ai) are equally spaced between the minimum and maximum values of the observed data for the month, whereas for the lengths of dry and wet series and for precipitation, the interval size gradually increases as i increases. In the latter two cases, there are typically many small values but also a few very large ones and this choice of interval structure prevents a very coarse resolution being used for the small values. (Semenov, Barrow, 2002).

Since radiation parameter does not follow normal distribution, a semi-empirical distribution based on the frequency of arid and humid days is used to replicate daily radiation. In this model, radiation is modeled independently of temperature. It is also possible to get rainfall of the intended month independently of humid series or the amount of rainfall of previous day. Daily maximum and minimum temperatures are modeled in the form of random processes and daily mean and standard deviation related to the humidity or aridity of the intended day. February series estimate temperature. That is, third rank February series is used for duplicating mean and standard deviation of seasonal temperature. The residual values obtained from subtracting average generated values from the monitored values are used to calculate time auto-correlation of maximum and minimum data. Process of generating artificial data is performed in three steps: calibration, evaluation, generating artificial data.

LARS-WG model can generate daily meteorology data in stationed scale for future points of study using meteorology data of statistical period and RCP output in a period similar to statistical and future period. Artificial generated data are similar to monitored data or defined scenario statistically. It should be investigated whether monitored data and model are from acceptable population. In this study, the model power in monitoring data was calculated using root mean square error and absolute error between monitored and modeled data. Absolute error and root mean square error are obtained using following equations: (Boani and Morid, 2005)

$$RMSE = \sqrt{\frac{1}{n}\sum_{1=1}^{n}(si - oi)^2} \quad (6)$$

$$MAE = \frac{1}{n}\sum_{1=1}^{n}(si - oi) \quad (7)$$

si and oi are modeled parameter and monitored parameter respectively including minimum and maximum temperature, rainfall, and radiation where i refers to months. In this method, the monthly average of observed meteorology data is compared with output data of the GCMs. After processing the trend of data, capability of 15 general circulation models of atmosphere was assessed using LARS-WG microscale model and weighted average method. (Boani and Morid, 2005)

$$W_G^m = \frac{1/(P_G^m - P_O^m)}{\sum_{G=1}^{15} 1/(P_G^m - P_O^m)} \quad (8)$$

P_G^m is the average of GCM data from the G series for month m, P_O^m is the average of observed data and W_G^m is the weight of GCM data.

There are two ways to deal with the problem of predicting future against uncertainty. The first method is uncertainty analysis (probability analysis) and the second is scenario analysis. In this study, the first method was used as a climate scenario under the 4.5 and 8.5 scenarios in the following way: each indicating properties of the greenhouse gas emissions, especially CO2, active chemical gases, aerosols, black carbon, land user data, and land surface coverage. For this purpose, at first, points for which there are CCDS data were determined and then points near the target area were separated and variance analysis was done in order to select the best points for extracting the required data of the area after examining the desired climate. Past and future data of temperature and rainfall in two scenarios of 4.5 and 8.8 for the confirmed points from the previous stage were generalized to the points of the studied area using weighted average method.

Weighted average is calculated by the following formula: $W_i = 1/(\text{distance from the adjacent point})^2$

$$\bar{x} = \frac{\sum_{i=1}^{n} w_i x_i}{\sum_{i=1}^{n} w_i} \quad (9)$$

$\bar{x}$: Value of the estimated point, x_i: value of the adjacent point, W_i: weight of the adjacent point

At first, rainfall ratio was calculated by dividing future rainfall to past rainfall and temperature difference was calculated by subtracting future temperature from past temperature and all was done using MS Excel.

Rainfall= future rainfall/past rainfall

Temperature= future temperature- past temperature

Accordingly, 21 deltas will be obtained for temperature and 12 for rainfall each month, which is the average monthly forecasting scenario for the next 30 years and the results will be entered into the intended scenario file.

Changing Radiation to Sunny Hours

One of the Lars input data is sunny hours and its output is radiation. The following formula is used for converting radiation to sunny hours:

$$Rg = Ro\left(\alpha + (1-\alpha)\, S/So\right) \quad (10)$$

Where, Rg is daily value of global radiation; R0 is daily value of radiation in a clean day; S indicates sunny hours; and So is maximum of sunny hours, and α is the fixed amount of formula.

$$Rg = RA\left(a + bn/N\right) \quad (11)$$

Where, Rg is daily value of global radiation; RA is daily value of radiation in a clean day measured sunny hours; N is determined day length; a is percentage of RA reaching the ground on a cloudy day and b is percentage of RA absorbed by cloud on a cloudy day.

Investigating Uncertainty

There is increasing realization of the importance of defining uncertainty in ecological models and classifications of the types of uncertainty have been made identify two sources of uncertainty: (a) that are found in models, their structure, and their parameter values, and (b) that are found in data, due to its quality and natural variability, and due to missing data (Turley and Ford 2009). Climate change estimates on small (regional and local) spatial scales are burdened with a considerable amount of uncertainty, stemming from several sources. For estimates based directly on global climate model (GCM) outputs, different levels of uncertainty are related to (i) the forcing scenarios (interscenario variability), (ii) the use of different GCMs (intermodal variability), and (iii) different realizations of one GCM Mixing some models can decrease uncertainty of model structure (Huth 2004).

Results

Investigating Trend

Results of Mann-Kendall test in previous years are shown in figure 3: minimum temperature with two positive changes in 1977 and 1986 and one negative change in 1983 and Maximum temperature with two positive changes in 1977 and 1985 and one negative change in 2000. Rainfall trend indicates its annual decrease. There was a positive change in 1977 with no change in drought trend.

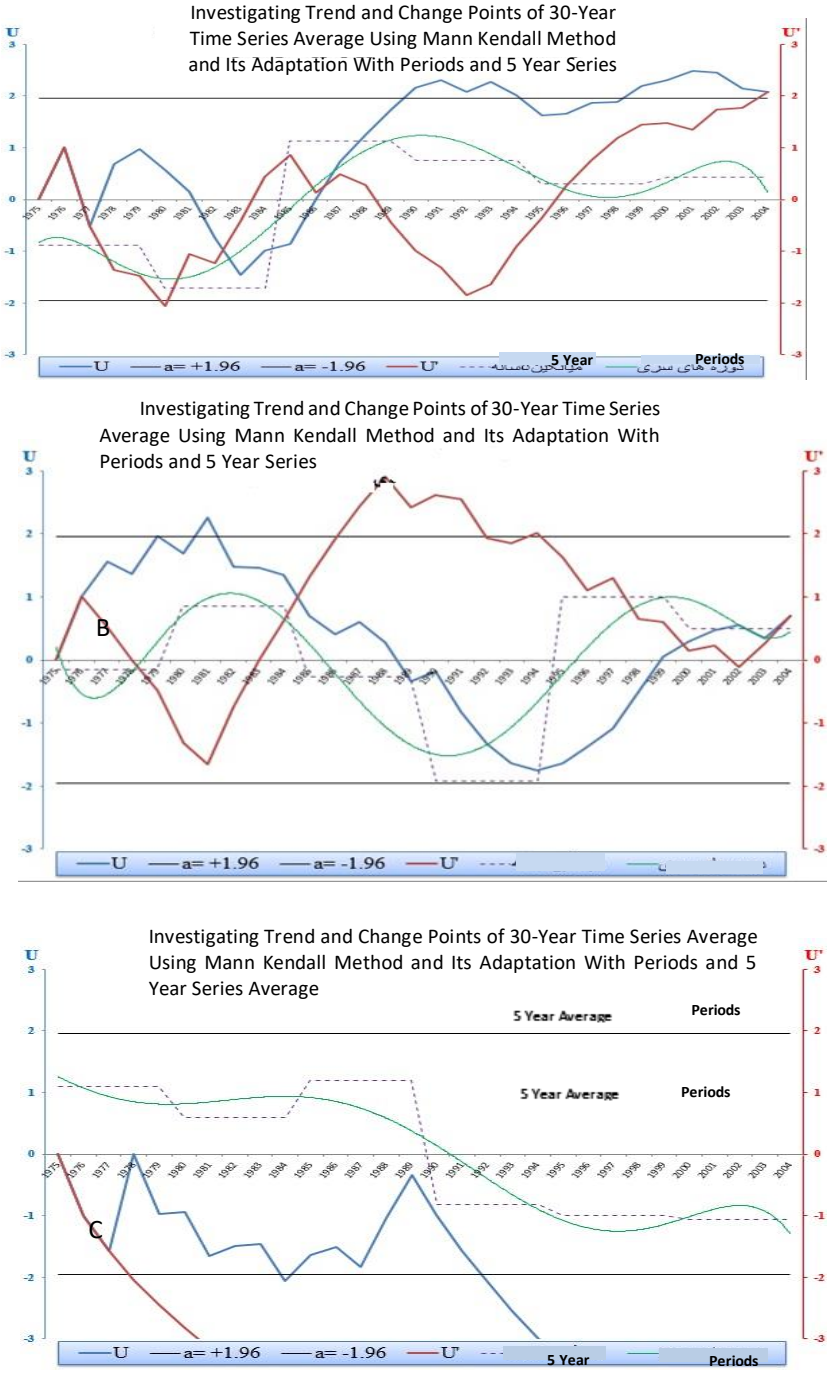

Fig. 3. Investigating Trend and Change Points of 30-Year(1975-2004) Time Series Average Using Mann Kendall Method and Its Adaptation With Periods and Year Series Average. A: Minimum Temperature, B: Maximum Temperature, C: Rainfall

According to Chart 3A, the trend of minimum temperature data from 1989 to 1949, and from 1999 to 2004, is a positive trend, and in the rest of the years data is not trendy. Also, from 1975 to 1970, the data series is static, while two positive mutations occurred in 1986 and 1977 and a negative mutation occurred in 1983. According to diagram 3B, there is no trend about the maximum temperature, and in 1975 to 1977 the static series occurred. A positive mutation was observed between 1977 and 2000 and a negative mutation in 1986, and there was a positive mutation in Fig. 3C of the precipitation trend in 1977 and has been decreasing since 1992.

Weighted Average

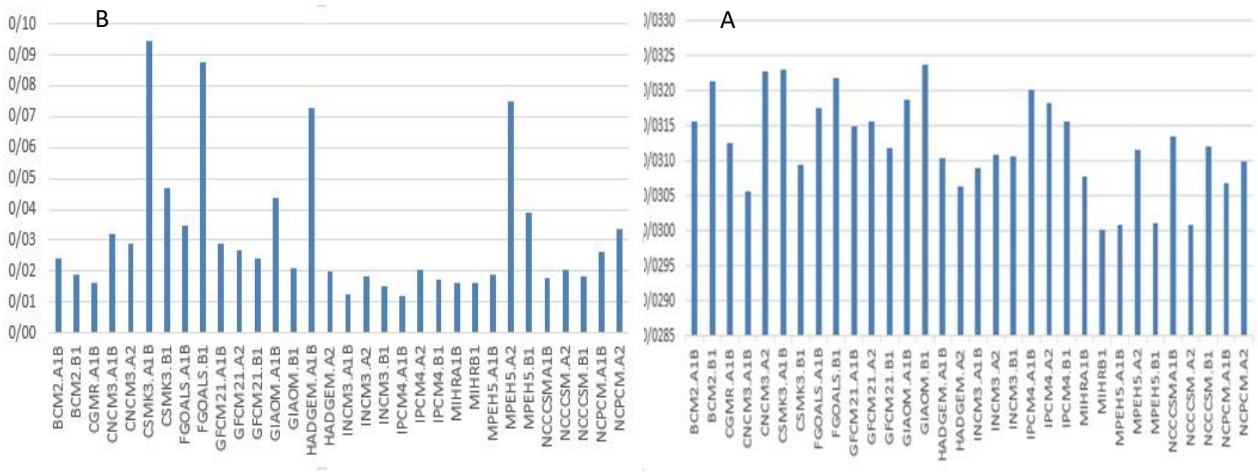

Fig. 4. A: Rainfall Weight B: Temperature Weight

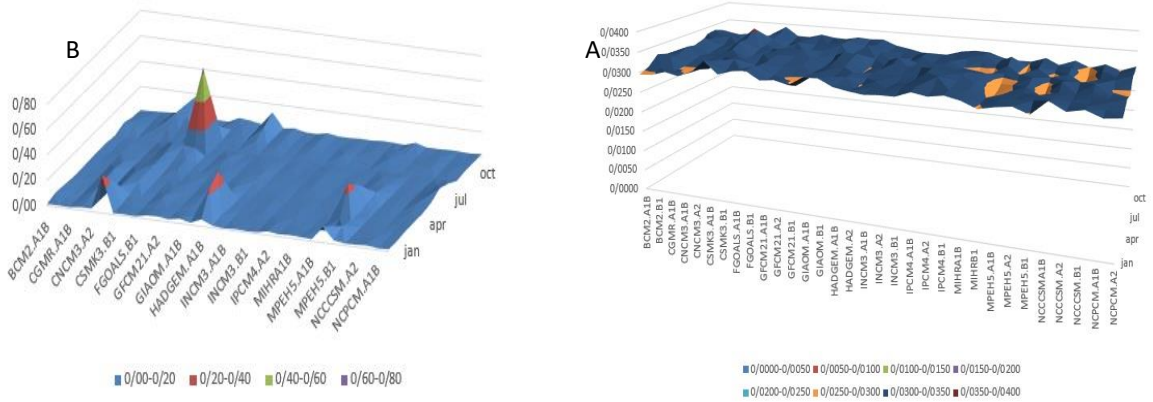

Fig. 5. Monthly rainfall weight (A) and temperature weight (B).

Results of figures 4 and 5 show that CSMK3 A1B ،FGOALS B1 ،HADGEM A1B ، MPEH5 A2 models are better for temperature and BCM2 B1 ، CSMK3 A1B , GIAOM B1 models are better for rainfall. Figure 5 shows that FGOALS B1 model will forecast the best in summer. Model capabilities are different from .01 to 50 in different months, so this study aimed at designing a model with high prediction power in almost all months.

Investigating Uncertainty

Results of Tables 4 and 5 show that INCM3.A1B, IPCM4.A1B are the best models in forecasting temperature and can forecast 1 ° increase in a month.

The worst model in forecasting temperature was MPEH5.B1. CSMK3.A1B and CNCM3.A2 are the most powerful models in predicting rainfall and predicts .0 decrease in rainfall and CSMK3.B1 is the weakest model which can predict 1 mm rainfall in a month. While temperature change in next 100 years will be 1- 2.5 ℃ and a decrease in rainfall based on IPCC forth report.

This difference in prediction is due to uncertainty of model and different scenarios. So, a mixed scenario was written for future prediction problem against uncertainty.

Table 4. The 2nd and the 4th Quarters of Temperature Predicted Data in Lars Model and Scenarios

GFCM21.A2	GFCM21.A1B	FGOALS.B1	FGOALS.A1B	CSMK3.B1	CSMK3.A1B	CNCM3.A2	CNCM3.A1B	CGMR.A1B	BCM2.B1	BCM2.A1B	quarters	
3/71	3/76	4/66	4/29	4/44	3/28	3/85	3/84	4/42	4/16	4/20	4th	JAN
3/52	3/54	3/99	3/80	3/88	3/30	3/58	3/58	3/87	3/74	3/76	2nd	
4/68	4/70	5/37	4/88	5/20	4/27	4/71	4/58	5/65	4/78	4/51	4th	FEB
4/45	4/46	4/80	4/55	4/71	4/25	4/47	4/40	4/93	4/50	4/37	2nd	
9/79	9/61	10/23	9/81	9/71	9/48	9/98	9/61	10/60	9/97	9/71	4th	MAR
9/56	9/47	9/78	9/57	9/52	9/40	9/65	9/47	9/96	9/65	9/52	2nd	
13/86	13/82	14/15	13/98	13/64	13/63	14/24	13/72	14/48	14/24	14/05	4th	APR
13/66	13/64	13/80	13/71	13/54	13/54	13/84	13/59	13/97	13/85	13/75	2nd	
18/47	18/55	18/58	18/60	18/30	18/30	18/76	18/33	19/00	18/96	18/76	4th	MAY
18/29	18/33	18/34	18/36	18/20	18/21	18/44	18/22	18/56	18/54	18/44	2nd	
22/59	22/58	22/45	22/54	22/33	22/47	22/85	22/46	22/89	22/92	22/74	4th	JUN
22/35	22/35	22/28	22/33	22/22	22/29	22/48	22/29	22/50	22/52	22/43	2nd	
26/18	26/06	25/81	25/86	25/74	26/00	26/58	26/21	26/12	26/32	26/13	4th	JUL
25/84	25/79	25/66	25/68	25/62	25/75	26/04	25/86	25/81	25/92	25/82	2nd	
25/10	25/01	24/59	24/56	24/57	24/76	25/39	25/24	25/04	25/23	24/96	4th	AUG
24/74	24/70	24/49	24/48	24/48	24/58	24/89	24/82	24/71	24/81	24/68	2nd	
22/55	22/52	21/84	21/93	22/05	22/10	22/49	22/48	22/55	22/47	22/22	4th	SEP
22/19	22/17	21/83	21/88	21/94	21/97	22/16	22/15	22/19	22/15	22/03	2nd	
17/47	17/50	16/99	17/14	17/12	17/17	17/17	17/21	17/48	17/25	17/17	4th	OCT
17/18	17/20	16/94	17/01	17/01	17/03	17/03	17/05	17/18	17/07	17/03	2nd	
11/71	11/76	11/82	11/81	11/57	11/49	11/46	11/65	11/85	11/76	11/90	4th	NOV
11/53	11/55	11/59	11/58	11/46	11/42	11/41	11/50	11/60	11/56	11/63	2nd	
6/32	6/27	7/05	6/85	6/59	5/94	6/34	6/53	6/67	6/85	7/09	4th	DEC
6/17	6/14	6/53	6/44	6/30	5/98	6/18	6/27	6/35	6/44	6/56	2nd	

MIHRB1	MIHRA1B	IPCM4.B1	IPCM4.A2	IPCM4.A1B	INCM3.B1	INCM3.A2	INCM3.A1B	HADGEM.A2	HADGEM.A1	GIAOM.B1	GIAOM.A1B	GFCM21.B1
3/93	3/84	3/96	3/73	4/40	4/57	4/20	5/04	4/05	3/54	4/04	3/65	3/93
3/63	3/58	3/64	3/52	3/86	3/94	3/76	4/18	3/69	3/43	3/68	3/48	3/62
5/18	4/94	5/00	4/68	5/36	5/24	5/27	5/64	4/61	4/18	4/87	4/75	4/87
4/70	4/58	4/61	4/45	4/79	4/73	4/75	4/93	4/41	4/20	4/54	4/48	4/55
10/52	10/33	10/03	10/12	10/56	10/02	10/32	10/38	10/00	9/36	9/81	9/73	9/99
9/92	9/83	9/68	9/72	9/94	9/67	9/82	9/85	9/66	9/34	9/56	9/52	9/65
14/36	14/35	14/11	14/32	14/75	14/10	14/30	14/45	14/17	13/66	13/88	13/78	14/07
13/91	13/90	13/78	13/89	14/10	13/77	13/88	13/95	13/81	13/56	13/66	13/61	13/76
18/82	18/90	18/83	18/88	19/27	18/80	18/84	18/98	18/65	18/40	18/58	18/44	18/61
18/47	18/50	18/47	18/50	18/69	18/45	18/47	18/54	18/38	18/26	18/34	18/27	18/36
22/84	23/00	22/83	22/76	23/05	22/87	22/88	22/91	22/56	22/54	22/65	22/47	22/56
22/47	22/56	22/47	22/44	22/58	22/49	22/50	22/51	22/33	22/33	22/38	22/29	22/34
26/20	26/42	26/19	26/08	26/34	26/38	26/36	26/47	25/99	26/05	26/17	25/96	25/92
25/86	25/97	25/85	25/79	25/92	25/95	25/93	25/99	25/75	25/78	25/84	25/74	25/72
25/12	25/19	25/05	25/00	25/26	25/33	25/17	25/43	24/99	24/94	25/09	24/98	24/76
24/76	24/79	24/72	24/69	24/83	24/86	24/78	24/91	24/69	24/66	24/74	24/69	24/58
22/70	22/63	22/44	22/34	22/74	22/67	22/44	22/69	22/50	22/40	22/47	22/41	22/34
22/26	22/23	22/14	22/09	22/28	22/25	22/13	22/26	22/16	22/11	22/15	22/12	22/09
17/76	17/64	17/60	17/33	17/82	17/52	17/35	17/62	17/59	17/34	17/49	17/23	17/55
17/32	17/26	17/25	17/11	17/35	17/21	17/12	17/25	17/24	17/11	17/19	17/06	17/22
12/12	11/99	12/30	12/03	12/36	12/02	11/73	12/24	12/31	11/75	11/98	11/49	11/89
11/74	11/67	11/82	11/69	11/85	11/68	11/54	11/79	11/83	11/55	11/66	11/42	11/62
6/66	6/60	6/87	6/76	7/09	7/05	6/52	7/37	7/21	6/47	6/72	6/12	6/48
6/34	6/31	6/44	6/39	6/55	6/53	6/27	6/70	6/62	6/24	6/37	6/07	6/25

NCPCM.A2	NCPCM.A1B	NCCCSM.B1	NCCCSM.A2	NCCCSMA1B	MPEH5.B1	MPEH5.A2	MPEH5.A1B
4/03	4/34	3/83	4/01	4/09	3/75	3/22	4/16
3/67	3/83	3/57	3/67	3/70	3/53	3/27	3/74
4/81	5/05	4/70	4/83	5/00	4/36	3/80	4/78
4/52	4/64	4/46	4/53	4/61	4/29	4/01	4/50
9/72	9/85	9/92	9/93	10/10	9/55	9/09	9/97
9/52	9/58	9/62	9/62	9/71	9/43	9/21	9/64
13/84	13/92	14/11	14/05	14/10	13/75	13/41	14/24
13/65	13/68	13/78	13/75	13/78	13/60	13/43	13/84
18/51	18/51	18/83	18/68	18/72	18/32	18/17	18/96
18/31	18/31	18/47	18/40	18/41	18/21	18/14	18/54
22/43	22/43	22/89	22/79	22/92	22/33	22/35	22/92
22/27	22/27	22/50	22/45	22/52	22/22	22/23	22/51
25/69	25/83	26/34	26/29	26/50	25/85	25/87	26/32
25/60	25/67	25/92	25/90	26/00	25/68	25/69	25/91
24/64	24/77	25/26	25/08	25/17	24/83	24/80	25/23
24/52	24/58	24/82	24/73	24/78	24/61	24/60	24/81
22/28	22/29	22/66	22/38	22/37	22/38	22/32	22/47
22/06	22/06	22/25	22/10	22/10	22/10	22/08	22/15
17/42	17/39	17/66	17/33	17/40	17/51	17/35	17/25
17/16	17/14	17/28	17/11	17/15	17/20	17/12	17/07
11/84	11/88	12/06	11/78	11/92	12/02	11/74	11/76
11/59	11/62	11/70	11/57	11/64	11/69	11/54	11/56
6/58	6/81	6/65	6/62	6/72	6/72	6/32	6/85
6/30	6/41	6/33	6/32	6/37	6/37	6/17	6/43

Table 5. The 2nd and the 4th Quarters of Predicted Rainfall Data in Lars Models and Scenarios.

CGMR.A1B	BCM2.B1	BCM2.A1B	Quarters	
26/90	27/83	28/09	4th	jan
26/60	28/29	28/22	2nd	
37/02	36/56	36/56	4th	feb
36/88	36/34	36/56	2nd	
35/56	32/86	32/48	4th	mar
35/52	31/51	32/29	2nd	
23/72	22/44	22/60	4th	apr
23/70	21/80	22/68	2nd	
7/12	6/68	7/06	4th	may
7/10	6/45	7/25	2nd	
1/49	1/40	1/51	4th	jun
1/50	1/35	1/56	2nd	
0/33	0/31	0/34	4th	jul
0/00	0/01	-0/02	2nd	
0/22	0/20	0/22	4th	aug
0/22	0/20	0/22	2nd	
2/99	2/98	2/99	4th	sep
2/96	2/97	3/00	2nd	
7/88	8/01	7/67	4th	oct
7/51	8/07	7/49	2nd	
21/20	21/44	20/69	4th	nov
20/26	21/56	20/32	2nd	
29/80	30/45	30/36	4th	dec
28/86	30/77	30/32	2nd	

HADGEM.A2	HADGEM.A1	GIAOM.B	GIAOM.A1B	GFCM21.	GFCM21.A2	GFCM21.A1B	FGOALS.B1	FGOALS.A1B	CSMK3.B1	CSMK3.A1B	CNCM3.A2	CNCM3.A1B
26/96	26/42	25/07	25/20	26/96	26/25	26/61	25/00	25/38	26/27	24/04	26/42	27/51
26/76	26/15	24/40	25/26	27/83	25/90	26/79	24/19	25/57	26/71	22/92	27/60	28/06
36/79	35/87	34/52	34/16	37/93	36/62	36/71	33/66	35/03	35/57	33/29	35/89	37/31
37/07	35/40	33/84	33/99	39/81	35/97	36/75	32/14	35/72	35/85	32/15	37/19	38/01
35/65	33/66	34/00	33/32	36/14	35/78	34/88	32/54	34/83	31/89	33/12	35/15	35/64
36/46	32/67	34/16	32/98	37/54	35/60	34/44	31/36	35/98	30/42	33/74	36/16	35/89
23/54	22/84	23/21	23/03	23/94	23/48	22/94	22/12	23/05	22/45	22/49	23/84	23/75
23/54	22/49	23/40	22/93	24/40	23/26	22/67	21/70	23/52	22/15	22/50	24/52	23/71
7/16	7/39	6/98	7/06	7/37	7/06	6/95	6/70	6/70	7/36	6/92	7/06	7/16
7/15	7/50	6/78	7/10	7/53	6/90	6/89	6/57	6/70	7/69	6/70	7/12	7/21
1/51	1/53	1/41	1/42	1/52	1/43	1/41	1/40	1/40	1/59	1/49	1/40	1/49
1/55	1/54	1/35	1/42	1/58	1/39	1/40	1/39	1/40	1/69	1/45	1/36	1/53
0/34	0/35	0/31	0/31	0/35	0/33	0/31	0/31	0/32	0/35	0/34	0/31	0/33
-0/01	0/00	0/02	0/00	-0/02	0/01	0/01	0/00	0/00	-0/02	0/01	0/02	-0/01
0/22	0/22	0/22	0/22	0/22	0/21	0/21	0/22	0/22	0/22	0/22	0/20	0/21
0/21	0/22	0/22	0/22	0/22	0/21	0/21	0/22	0/22	0/21	0/22	0/19	0/21
3/23	3/10	2/95	3/29	2/99	3/01	3/17	3/27	3/34	3/27	3/15	2/78	3/07
3/16	3/03	2/87	3/46	2/84	3/01	3/24	3/32	3/37	3/24	3/09	2/60	3/21
8/55	8/29	7/84	8/38	7/68	7/99	8/60	8/61	8/06	8/61	7/99	7/88	8/63
8/60	8/16	7/61	8/65	7/33	8/14	8/90	8/62	7/78	8/89	7/67	7/82	9/00
22/09	21/83	20/95	21/44	20/33	21/05	21/76	21/92	21/43	21/97	20/50	21/11	23/06
22/03	21/69	20/51	21/69	19/77	21/42	22/11	22/01	21/18	22/24	19/76	21/42	24/03
30/43	29/86	28/62	28/80	28/62	29/27	29/15	28/63	29/51	29/47	27/47	29/10	31/67
30/05	29/58	28/01	28/89	28/53	29/59	29/09	28/37	29/95	29/45	26/47	29/92	32/96

NCCCSM.	NCCCSM.	NCCCSMA	MPEH5.B	MPEH5.A	MPEH5.A1B	MIHRB1	MIHRA1B	IPCM4.B1	IPCM4.A2	IPCM4.A1B	INCM3.B1	INCM3.A2	INCM3.A1B
25/90	26/55	25/03	27/82	26/62	27/07	27/81	26/51	25/90	26/39	25/90	27/05	27/08	27/34
25/31	26/88	24/27	29/21	26/02	27/29	28/18	25/85	25/59	26/64	25/65	27/63	27/09	27/47
35/33	35/82	34/55	35/30	35/60	35/87	37/01	35/68	34/72	35/21	34/56	35/60	35/98	36/22
35/11	36/07	33/92	35/68	35/74	36/00	37/59	35/01	34/23	35/46	34/23	36/13	36/16	36/34
34/37	34/20	33/74	33/65	34/39	34/85	35/42	33/74	33/24	31/52	32/69	34/00	34/80	34/03
34/69	34/11	33/50	33/60	34/76	35/08	35/71	32/91	32/99	30/65	33/28	34/65	35/20	33/64
23/28	23/57	23/36	23/59	23/47	23/89	24/81	22/79	22/41	21/83	21/63	23/75	23/90	23/54
23/36	23/72	23/26	23/70	23/41	24/10	25/27	21/78	22/22	21/53	21/53	24/80	23/98	23/36
7/07	7/27	7/26	7/70	7/14	7/47	7/87	7/13	6/80	6/75	6/65	7/19	7/22	7/19
7/01	7/36	7/26	7/91	6/86	7/64	8/07	6/75	6/63	6/73	6/60	7/47	7/23	7/18
1/43	1/49	1/43	1/60	1/49	1/52	1/62	1/49	1/43	1/43	1/40	1/42	1/43	1/41
1/38	1/52	1/41	1/68	1/44	1/54	1/67	1/43	1/39	1/43	1/39	1/42	1/43	1/40
0/33	0/33	0/33	0/35	0/33	0/35	0/35	0/33	0/33	0/33	0/33	0/33	0/33	0/31
0/01	0/00	0/00	-0/01	0/01	-0/01	0/00	0/01	0/00	0/00	0/00	0/00	0/00	0/01
0/22	0/23	0/22	0/22	0/22	0/22	0/22	0/23	0/22	0/22	0/22	0/22	0/22	0/22
0/22	0/23	0/22	0/22	0/22	0/22	0/22	0/23	0/22	0/22	0/21	0/22	0/22	0/22
3/29	3/58	3/24	3/42	3/17	3/44	3/16	3/44	3/46	3/32	3/17	3/20	3/11	3/38
3/33	3/72	3/07	3/51	3/04	3/57	3/02	3/58	3/47	3/26	3/10	3/22	3/07	3/51
8/24	9/08	8/23	8/42	8/12	8/81	7/82	8/42	8/25	8/15	8/23	8/24	8/03	8/46
8/14	9/50	7/80	8/52	7/97	9/16	7/33	8/72	8/16	8/10	8/27	8/25	7/92	8/68
21/80	23/87	22/15	22/03	21/37	22/70	21/81	22/28	21/08	21/23	21/60	21/95	21/80	22/22
21/45	24/91	21/28	21/97	21/04	23/36	21/37	22/52	20/48	21/31	21/78	22/12	21/72	22/43
30/27	31/49	29/96	31/65	29/92	31/15	31/85	30/78	29/66	29/54	30/00	31/26	31/29	31/19
29/63	32/09	29/19	32/50	29/05	31/77	32/20	30/24	29/10	29/48	30/24	31/89	31/30	31/14

NCPCM.A1	27/07	27/26	35/76	35/64	33/74	33/58	23/12	23/23	7/19	7/19	1/52	1/52	0/35	0/00		0/22	0/22	3/20	3/24	8/43	8/53	22/48	22/91	31/56	32/24
NCPCM.A2	26/68	26/68	35/99	35/99	34/05	34/05	22/91	22/91	7/21	7/21	1/53	1/53	0/35	0/00		0/22	0/22	3/13	3/13	8/23	8/23	21/62	21/62	30/18	30/18

LARS WG Model Deduction

Tables 1 and 3 show the results of model deduction using RMSE, MAE, R^2 error indicators. Based on the values, model is appropriate for predicting climate change in Pol-Kalle Station.

Table 6. MAE and RMSE Error Results in Lenjanat Watershed.

station	Sunny hours	Maximum temperature	Minimum temperature	rainfall	statistics
Lenjanat	0.9999	0.9936	0.9945	0.9892	R^2
	0.1315	0.7145	0.6526	2.1535	RMSE
	0.1233	0.6075	0.5808	1.67	MAE

As table 5 shows, determination coefficient value is significant for all parameters. Error indicators are relatively low, showing relative and acceptable adaptation of simulation by the model and observed values of the fundamental period. Model capability in generating data, therefore, was confirmed and data were subsequently simulated for next 30 years. Precision and validity of past data in predicting future was done on Lars-WG software by P-value, F, and T. The highest precision and validity of data for rainfall was in January, June, and November and for temperature was in January, and for radiation was in May. Based on the results of Table 6 and 7 and figure 6, temperature, rainfall, and radiation data are capable of predicting future. Figure 6 shows that highest rainfall was in December and March and the least was in June and September. The lowest value of minimum and maximum temperature was in July, and the highest value was in January. The highest radiation, however, was in June and the lowest was in January and December. All data confirm each other and there is a significance effect between radiation and temperature and a negative relationship between these two parameters and temperature.

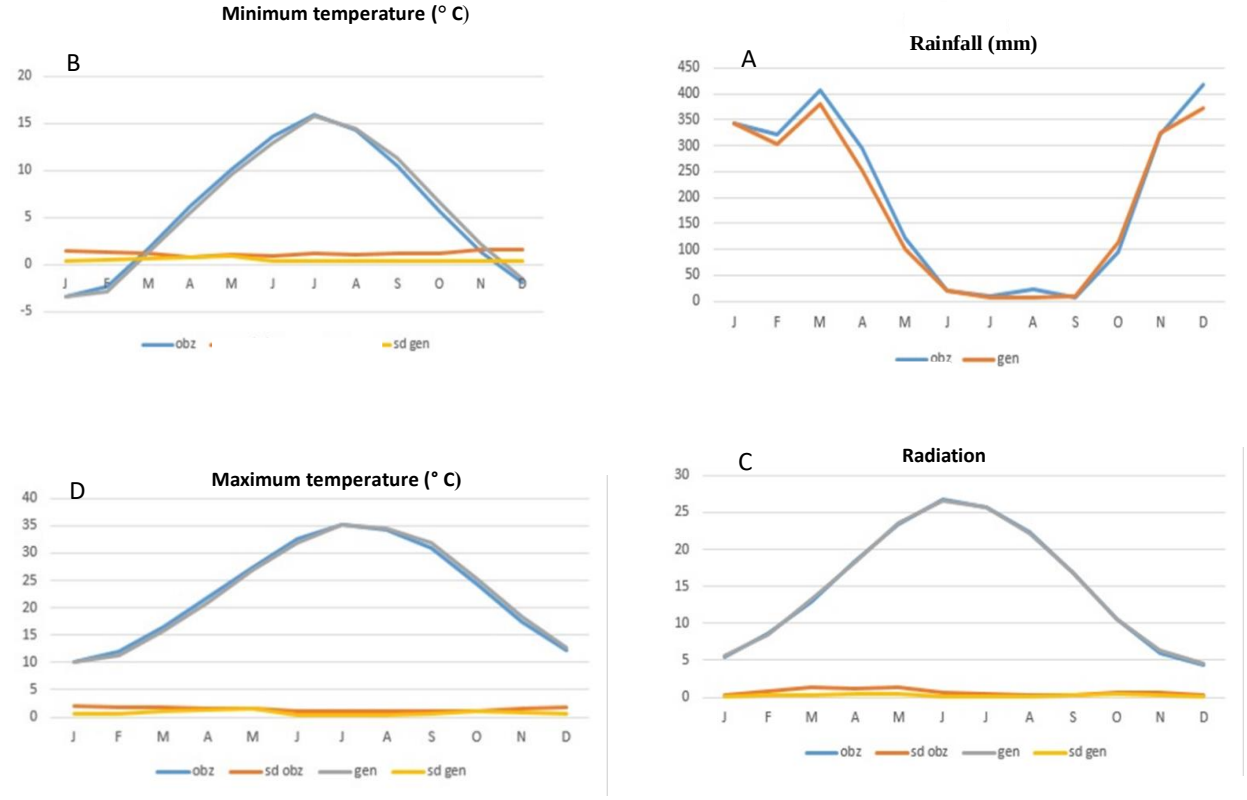

Fig. 6. Data Comparison: rainfall (A), minimum temperature (B), radiation (C), and maximum generated and observed temperature (D).

Table 8. P- Value for rainfall, minimum temperature, maximum temperature, and radiation predicting future climate

	J	F	M	A	M	J	J	A	S	O	N	D
rainfall	0.39	0.61	1.00	1.00	1.00	0.51	0.99	0.49	0.86	1.00	1.00	0.66
Minimum temperature	1.00	0.64	0.63	0.91	0.91	0.63	1.00	1.00	0.91	0.91	1.00	1.00
Maximum temperature	1.00	0.91	0.91	0.91	1.00	0.64	1.00	1.00	0.91	1.00	1.00	1.00
radiation	0.98	1	1	1	1	1	1	1	1	1	1	1

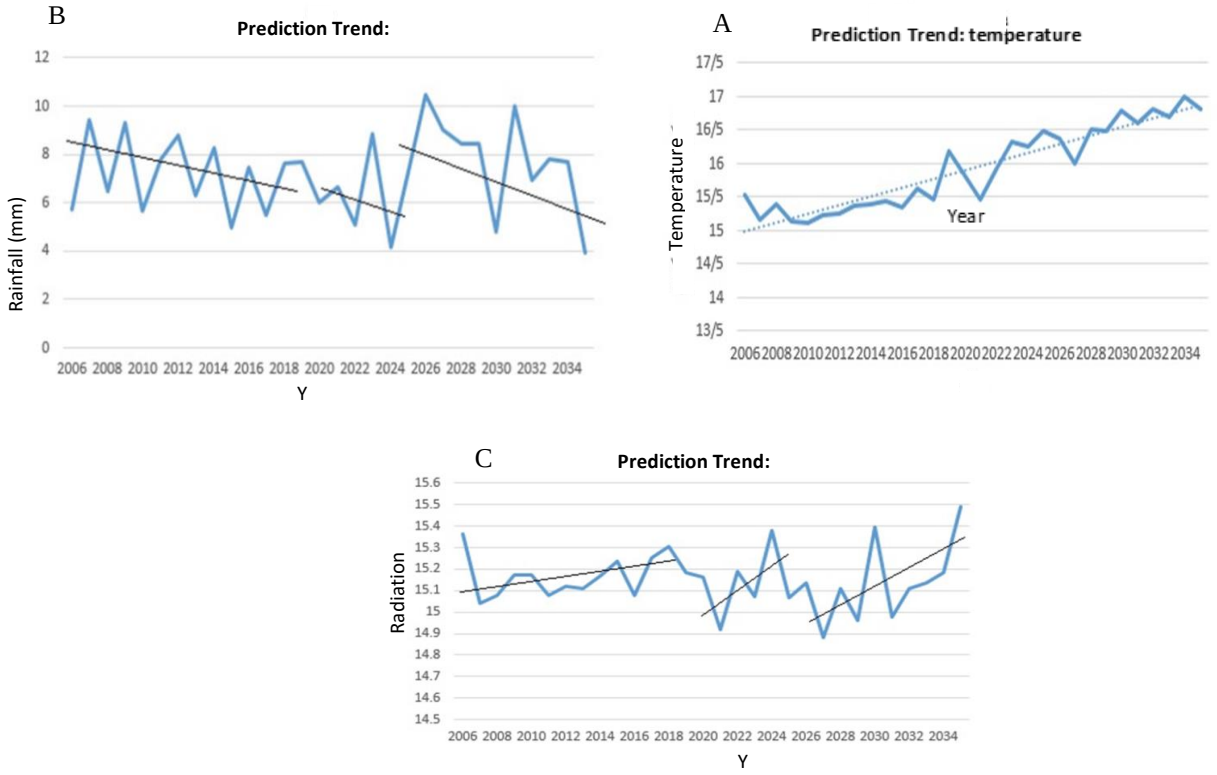

Fig. 7. Prediction Trend for average temperature (A), rainfall (B), and radiation (C) in 2005-2035 period in RCP 4.5 scenario.

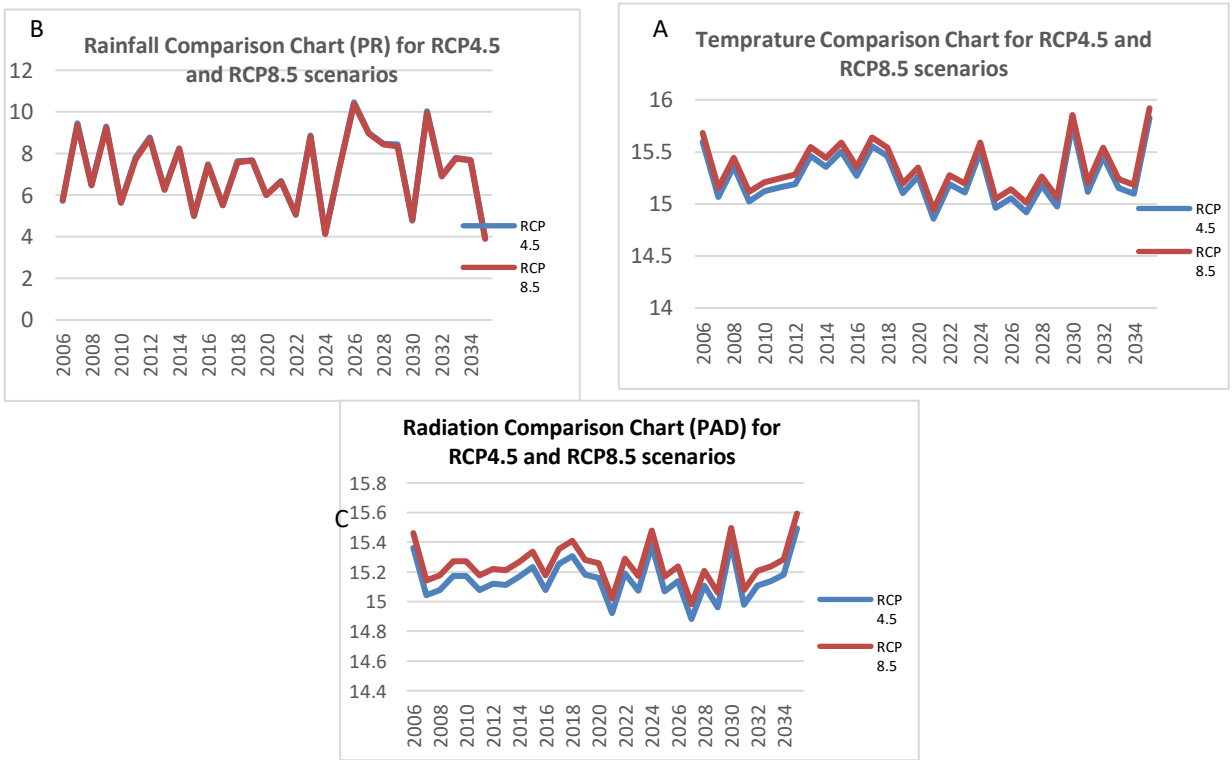

Fig. 8. Comparison chart for RCP4.5 and RCP8.5 scenarios towards average temperature (A), rainfall (B), and radiation (C) in 2005-2035

Lars results in scenarios RCP 4.5 and RCP 8.5 had temperature increase about 2.5 and 3.5 ℃ and rainfall decrease about 0.9 and 1.03 till 2035.

In the 8.5 scenario, due to population growth, industrial development and, in addition, greenhouse gas emissions, droughts, etc., there is a higher warming and lower rainfall than the 4.5 scenario, fluctuations in the graphs are due to years of aging between droughty years, but in total The drought trend is expected to continue.

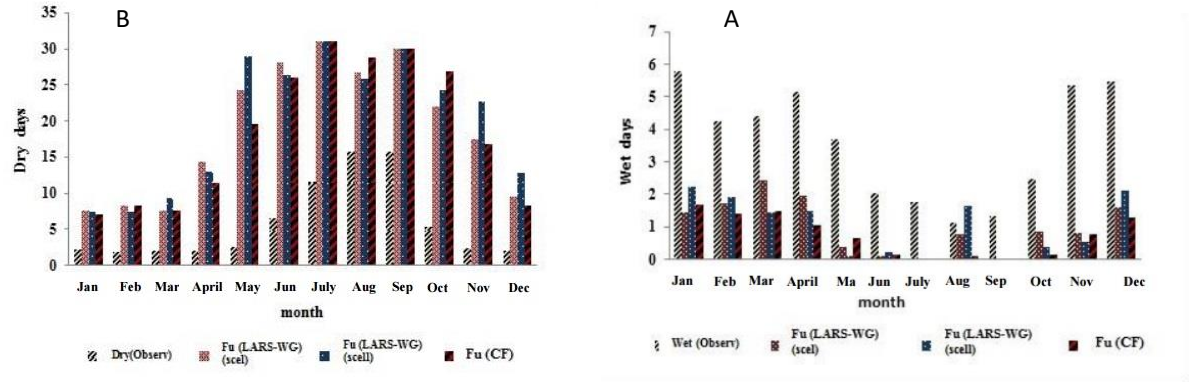

Fig. 9. Frequency average of observed humid days (A), predicted arid days (B), and factor change scenario

As the results of Figure 10 show, humid days are decreasing and arid days are increasing. The highest decline of humid days was in November and increase in arid days was in May. A further decline in humid days and further increase in dry days occurred in pessimistic scenario. Results of correlation test is a high and direct correlation between rainfall and river flow and underground water was 97% and 95% respectively and negative correlation between temperature average and radiation with underground water level was 93% and 87% respectively. There will be a problem in providing future surface water and underground water due to warming increase and rainfall decrease.

Discussions

This study aims at investigating local changes due to climate change from 2005 to 2035 AD in Lenjanat watershed. So, output data of general circulation models of atmosphere are downscaled with two climate change scenarios 8.5 and 4.5 with LARS-WG model in Pol-Kalle Station. The results of that synoptic station were assessed for the basic period 1975-2005 and the future period of 2005-2035. To assess the model power, root mean square error and absolute error were calculated between monitored and modeled data.

Before running the model for predicting future, precision and validity of results were assessed. The highest precision and validity for rainfall was in January, June, and November and the highest radiation was in May.

Investigating results of Mann-Kendall test in recent years shows that minimum temperature had two positive changes in 1977 and 1986 and a negative change in 1983. The two positive changes of maximum temperature were in 1977 and 1985, with a negative change in 2000. Rainfall trend has been declining every year in recent years. Of course, a positive change occurred 1977, which did not change the drought trend.

Results show that the highest rainfall was in December and March, and the lowest was in June-September. Also, the lowest minimum and maximum temperatures were in July and the highest in January. The highest radiation was in June and the lowest was in January and December.

Model was appropriate for Lenjanat watershed. The results show that rainfall is decreasing; the minimum and maximum temperatures in both scenarios are increasing and the frequency of humid days is decreasing while the frequency of arid days is increasing. The highest decline of humid days was in November and increase in arid days was in May. A further decline in humid days and further increase in arid days occurred in pessimistic scenario. All of the data confirm each other and show a significant relationship between the observed temperature and air temperature and negative relationship between the two parameters and rainfall.

References

Abbasi, F., Malboosi, Sh., Babaian, A., Asmari, M., Borhani, R. (2010). Predicting climate change in south Khorasan from 2010 to 2039 using exponential statistical microscale of G-ECHO model output. J of Soil and Water, 24, 218-233.

Babaian, A., ZooNajafi, N. (2006). Assessing WG–LARS model foe modeling meteorology parameters in Khorasan province. Nivar J, 62, 49-65.

Massah Boani, A., Morid, S. (2005) Climate Change Effects on Water Resources and Crop Production. Ir J Water Resour Res 40.

MehdiZadeh, P., Meftah Haghighi, M., Sayed Qasemi, S., Mosaedi, A. (2011) Investigating the effect of climate change on rainfall in Golestan Dam basin. J Water and Soil Conservation Studies,18, 117-132.

Cox, D. R., & Stuart, A. (1955). Some quick sign tests for trend in location and dispersion. Biometrika, 42(1/2), 80-95.

Guo, J., Chen, H., Xu, C. Y., Guo, S., & Guo, J. (2012). Prediction of variability of precipitation in the Yangtze River Basin under the climate change conditions based on automated statistical downscaling. Stochastic environmental research and risk assessment, 26(2), 157-176.
Hamed, K. H. (2008). Trend detection in hydrologic data: the Mann–Kendall trend test under the scaling hypothesis. Journal of hydrology, 349(3), 350-363.
Hamed, K. H., & Rao, A. R. (1998). A modified Mann-Kendall trend test for autocorrelated data. Journal of Hydrology, 204(1-4), 182-196.
Hasheminasab Khaybazi, F., Mousavi Baghi, M., Bakhtiari, B., Davari, K. (2013) Estimating rainfall change in the province of Kerman over the next 20 years using HADCM3 micro-scaling models. Irani J Irrigation and Water Engineering, 12, 43- 58.
Huth, R. (2004). Sensitivity of local daily temperature change estimates to the selection of downscaling models and predictors. Journal of Climate, 17(3), 640-652.
Khazanedari, L., Zabolabasi, F., Qandehari, Sh., Kohi, M., Malbosi, Sh. (2009) Perspective of the drought situation in Iran over the next thirty years. J Geography and Regional Development, 12, 83-98.
Khaliq, M. N., Ouarda, T. B., Gachon, P., Sushama, L., & St-Hilaire, A. (2009). Identification of hydrological trends in the presence of serial and cross correlations: A review of selected methods and their application to annual flow regimes of Canadian rivers. Journal of Hydrology, 368(1), 117-130.
Meshkatee, A., Kordjazi, M., Babaian, I. (2010) Evaluating and investigating Lars model in the simulation of meteorological data in Golestan province during 1993-2007. Ir J.Geography, 16, 81-96
Massah Bevani, A., Morid, S. (2005). Impact of climate change on water resources and agricultural products Journal of Sciences and Technology of Agriculture and Natural Resources (jstnar), 4, 17-28
MehdiZadeh, S., Moftah Haghighi, M., Sayed Qasemi, S., Mosaedi, A. (2011). Investigating the impact of climate change on rainfall in Golestan Dam Basin. Journal of Water and Soil Conservation Studies, 18(3), 117-132.
Salon, S., Cossarini, G., Libralato, S., Gao, X., Solidoro, C., & Giorgi, F. (2008). Downscaling experiment for the Venice lagoon. I. Validation of the present-day precipitation climatology. Climate Research, 38(1), 31-41.
Sang, Y.-F., Wang, Z., Liu, C. (2014). Comparison of the MK test and EMD method for trend identification in hydrological time series. J. Hydrol, 510, 293-298.
Semenov, M.A., Barrow, E.M. (2002). LARS-WG a stochastic weather generator for use in climate impact studies. User's manual, Version 3.0.
Trigo, R. M., & Palutikof, J. P. (2001). Precipitation scenarios over Iberia: a comparison between direct GCM output and different downscaling techniques. Journal of Climate, 14(23), 4422-4446.
Turley, M. C., & Ford, E. D. (2009). Definition and calculation of uncertainty in ecological process models. Ecological Modelling, 220(17), 1968-1983.
Von Storch, H. (1999). Misuses of statistical analysis in climate research (pp. 11-26). In Analysis of Climate Variability. Springer. Berlin. Heidelberg.

Citation:
Afrooz Bagheri, Bahram Malek Mohammadi, Banafsheh Zahraie, Amir Hessam Hasani, Farzam Babaie (2018). Assessment of uncertainty associated with precipitation and temperature predictions: climate change impact assessment in Lenjanat Watershed, Central Iran. *Ukrainian Journal of Ecology, 8*(1), 194–210.